

Research article

Lingbo Xia, Biao Yang, Qinghua Guo, Wenlong Gao, Hongchao Liu, Jianguang Han, Weili Zhang and Shuang Zhang*

Simultaneous TE and TM designer surface plasmon supported by bianisotropic metamaterials with positive permittivity and permeability

<https://doi.org/10.1515/nanoph-2019-0047>

Received February 18, 2019; revised April 5, 2019; accepted April 11, 2019

Abstract: Surface plasmon polaritons (SPPs) are surface modes existing at the interface between a metal and a dielectric material. Designer SPPs with a customer-defined property can be supported on the surface of suitably engineered metallic structures. They are important for various applications, ranging from chemical sensing to super-resolution imaging. In conventional systems, SPPs are transverse magnetic (TM) polarized, because of their origin in the collective electron oscillation along the surface. In this work, we show that both transverse electric (TE) and TM designer surface plasmons can be supported at the interface between a suitably designed bianisotropic metamaterial and a normal dielectric material without involving either negative permittivity or negative permeability. We

further propose a realistic bianisotropic metamaterial for implementation of the double surface modes. The bianisotropic metamaterial demonstrated here may have tremendous applications in optical information processing and integrated photonic devices.

Keywords: metamaterials; surface plasmon.

1 Introduction

Surface plasmon polariton (SPP) supported at the interface between a metal and a dielectric material has attracted enormous interest due to its wide applications including super-resolution imaging [1–5], cloaks [6–9], holography [10–15], etc. The intensity of SPP reaches a maximum right at the interface, and it decays into both the metal and the dielectric on both sides of the interface. Traditionally, it was believed that SPPs exist only at optical frequencies where the electromagnetic wave has non-negligible penetration into the metal. At lower frequencies such as microwave frequencies, most metals function as nearly perfect electric conductors and, therefore the SPP appears more like a half-space plane wave, having negligible penetration into the metal and almost no decay on the dielectric side. In 2004, Pendry proposed that structured metals can support a designer (spoof) plasmon at the interface, with the effective plasma frequency controlled by the geometry [16]. This work expands the study of SPPs from optical frequencies to the terahertz [17–19] and microwave regimes [1, 7, 20]. It is well known that the SPP is a transverse magnetic (TM) wave, with its magnetic field parallel to the interface, while the electric field has both components perpendicular to the interface and along the propagation direction. Interestingly, due to the transverse nature of the electromagnetic wave, the electric field of the SPP exhibits an interesting spin texture [21, 22], with the spin defined by $\mathbf{S} = \frac{\text{Re}\mathbf{k} \times \text{Im}\mathbf{k}}{(\text{Re}\mathbf{k})^2}$, always lying in the plane but perpendicular to the propagation direction of the SPP. This so called spin-orbit locking [23] is considered an optical analog

*Corresponding author: **Shuang Zhang**, School of Physics and Astronomy, University of Birmingham, Birmingham B15 2TT, UK, e-mail: s.zhang@bham.ac.uk

Lingbo Xia: Center for Terahertz Waves and College of Precision Instrument and Optoelectronics Engineering, Tianjin University and the Key Laboratory of Optoelectronics Information and Technology (Ministry of Education), Tianjin 300072, China; and School of Physics and Astronomy, University of Birmingham, Birmingham B15 2TT, UK

Biao Yang: School of Physics and Astronomy, University of Birmingham, Birmingham B15 2TT, UK; and College of Advanced Interdisciplinary Studies, National University of Defense Technology, Changsha 410073, China

Qinghua Guo, Wenlong Gao and Hongchao Liu: School of Physics and Astronomy, University of Birmingham, Birmingham B15 2TT, UK

Jianguang Han: Center for Terahertz Waves and College of Precision Instrument and Optoelectronics Engineering, Tianjin University and the Key Laboratory of Optoelectronics Information and Technology (Ministry of Education), Tianjin 300072, China

Weili Zhang: Center for Terahertz Waves and College of Precision Instrument and Optoelectronics Engineering, Tianjin University and the Key Laboratory of Optoelectronics Information and Technology (Ministry of Education), Tianjin 300072, China; and School of Electrical and Computer Engineering, Oklahoma State University, Stillwater, OK 74078, USA

of the quantum spin Hall effect of the electronic system, which has been extensively studied in solid-state systems. As the SPP decays away from the interface in both the dielectric and the metal, it follows that the rotation direction of the electric field is opposite across the interface, as schematically illustrated in Figure 1A and B. Since the boundary condition dictates that the in-plane electric field is continuous across the interface, the normal components of the electric field must be opposite to each other due to the opposite spins across the interface, and therefore the dielectric constants of the two media must be opposite to each other. By applying the same argument to transverse electric (TE) polarization at the interface between two different isotropic media, the condition for the existence of the surface mode is that the magnetic permeabilities must be opposite to each other across the interface. Thus, it simply follows that both TE and TM surface plasmons can coexist at the interface of a normal dielectric material

and a double negative medium (DNM) with simultaneous negative permittivity and permeability [20, 24, 25]. Despite a number of theoretical investigations into this possibility, the experimental implementation of the system [26–28], however, has not been achieved due because of the complexity involved in realizing isotropic DNMs. In this paper, we show that both TE and TM surface modes can be supported at the surface of a suitably designed bianisotropic material without involving either negative permittivity or negative permeability, as schematically illustrated in Figure 1C, which represents a much more viable approach than with DNMs.

2 Results

Bianisotropy refers to a coupling between the electric and magnetic responses along orthogonal directions. The

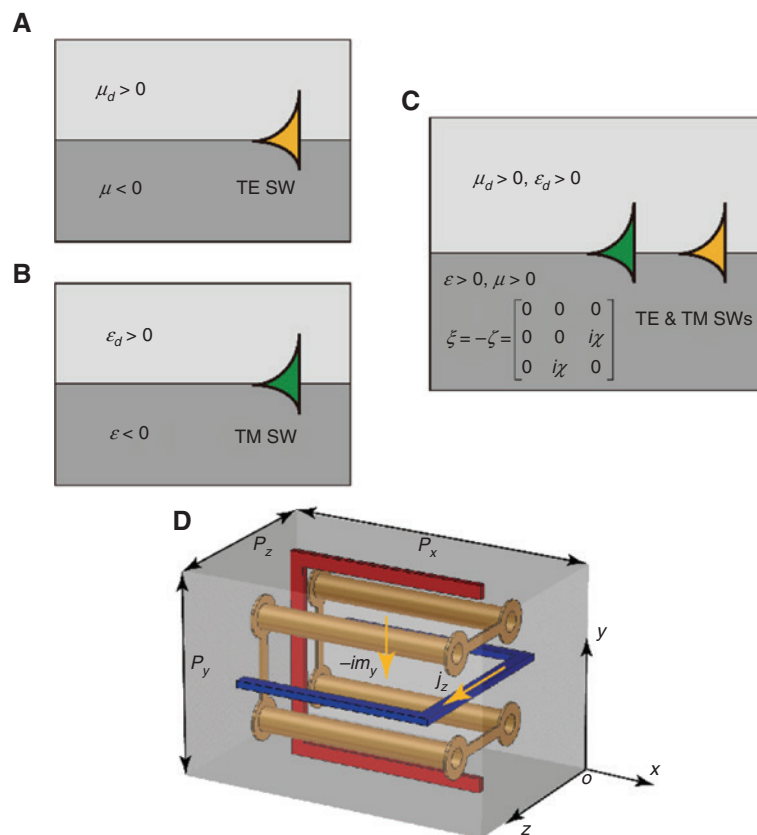


Figure 1: Schematic illustration of three types of interface with corresponding surface wave and one realistic model of bianisotropic metamaterial.

(A) TE surface wave in a ferromagnet/dielectric interface. (B) TM surface wave at the metal/dielectric interface. (C) TE and TM surface waves coexist in a bianisotropic material/dielectric interface. (D) Unit cell of a bianisotropic metamaterial. The copper solid represents copper and the light gray region is filled with dielectric material (F4BM) with relative permittivity $\epsilon = 2.2$. The copper structure is identical to two split-ring resonators, denoted by red and blue. The bianisotropic response can be understood from the field and current coupling between the two split-ring resonators. The periods in the x -, y -, and z -directions are $P_x = 4.67$ mm, $P_y = 3$ mm, and $P_z = 3$ mm. Details of the parameters can be found in the CST file in Supplementary Information.

constitutive equation in view of the coupling between electric and magnetic response is given by [29]

$$\mathbf{D} = \boldsymbol{\varepsilon}\mathbf{E} + \boldsymbol{\xi}\mathbf{H} \quad \mathbf{B} = \boldsymbol{\mu}\mathbf{H} + \boldsymbol{\zeta}\mathbf{E} \quad (1)$$

where $\boldsymbol{\varepsilon}$ and $\boldsymbol{\mu}$ are the permittivity and permeability, respectively, and $\boldsymbol{\xi}$ and $\boldsymbol{\zeta}$ are the coupling coefficients between the electric and magnetic fields. In general, all the coefficients are 3×3 tensors when anisotropy is present. Assuming that both the permittivity and permeability tensors are diagonal and the coupling between the electric and magnetic field only exist in y - z direction, the constitutive parameters can be expressed as

$$\boldsymbol{\varepsilon} = \begin{pmatrix} \varepsilon_{xx} & 0 & 0 \\ 0 & \varepsilon_{yy} & 0 \\ 0 & 0 & \varepsilon_{zz} \end{pmatrix}, \quad \boldsymbol{\mu} = \begin{pmatrix} \mu_{xx} & 0 & 0 \\ 0 & \mu_{yy} & 0 \\ 0 & 0 & \mu_{zz} \end{pmatrix} \quad (2)$$

$$\boldsymbol{\xi} = \boldsymbol{\zeta}^+ = \begin{pmatrix} 0 & 0 & 0 \\ 0 & 0 & i\gamma \\ 0 & i\gamma & 0 \end{pmatrix}$$

Here we consider an interface in the y - z plane formed between a normal dielectric material ($x > 0$) and the bianisotropic material ($x < 0$) described above. The bianisotropic metamaterial possesses properties akin to those of a noble metal for the TM mode and of a ferromagnetic material for the TE mode. To better illustrate

the importance of bianisotropy, we set $\varepsilon_{xx} = \varepsilon_{yy} = \varepsilon_{zz} = \varepsilon$, $\mu_{xx} = \mu_{yy} = \mu_{zz} = \mu$. (Note that this assumption will simplify the analysis but is not essential for achieving TE and TM modes simultaneously.) In addition, we consider the case where the surface plasmon propagates along a certain high-symmetry direction (y -axis), such that on each side of the interface each surface mode consists only of a single evanescent component. This is in contrast to case of the Dyakonov wave [30] supported at the interface between a normal dielectric material and an anisotropic dielectric material, where the surface mode consists of two evanescent components on each side of the interface, i.e. TE and TM components on the normal surface side, and ordinary and extraordinary components on the anisotropic material side. The complete expression for the TM and TE surface modes on two sides of interface can be obtained by solving the Maxwell equation [31]. With the continuity of the tangent electrical field and the tangent magnetic field, we obtain the following equations for the TE and TM surface modes [bianisotropic metamaterial (ε, μ, γ) and dielectric material interface ($\mu_d = 1, \varepsilon_d$)] (see Supplementary Material):

$$\begin{cases} \frac{-\gamma + \sqrt{q^2 + \gamma^2 - \varepsilon\mu}}{\varepsilon} = -\frac{\sqrt{q^2 - \varepsilon_d}}{\varepsilon_d} & \text{TM} \\ \frac{\mu(\gamma + \sqrt{q^2 + \gamma^2 - \varepsilon\mu})}{q^2 - \varepsilon\mu} = -\frac{1}{\sqrt{q^2 - \varepsilon_d}} & \text{TE} \end{cases} \quad (3)$$

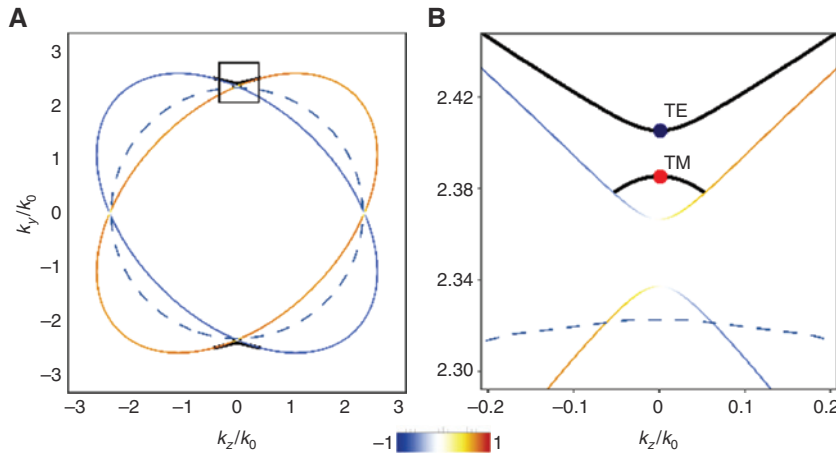


Figure 2: Dispersion of the bulk and surface wave of the bianisotropic metamaterial.

(A) Two ellipsoids denoting the two bulk mode EFS of the bianisotropic material with the parameters $\boldsymbol{\varepsilon} = \text{diag}(5.89, 6.79, 6.79)$, $\boldsymbol{\mu} = \text{diag}(1, 1.13, 1.13)$, and $\gamma = 1.16$ at 8.7 GHz. Its color denotes the degree of polarization, as shown in the color bar, with 1 and -1 denoting left-handed and right-handed circular polarization, respectively. The dashed blue line gives the bulk EFS of the dielectric material with permittivity $\varepsilon_d = 5.4$. The four black lines in the shape of two hyperbolas illustrate the surface wave existing between the interface of the bianisotropic material and the dielectric material. (B) Enlarged picture of the black dashed rectangle in (A). The highlighted blue and red points denote pure TE and TM surface modes, respectively.

where q denotes the wave vector (all the wave vectors in this paper are normalized to that in vacuum), and ε_d represents the permittivity of dielectric material. To have a physical solution, $q^2 - \varepsilon_d$ and $q^2 + \gamma^2 - \varepsilon\mu$ should be positive and $q^2 - \varepsilon\mu$ should be negative. We conclude that both TE and TM surface plasmons can exist when $\gamma > 0$ and $\varepsilon\mu > \varepsilon_d$. Also, the wave vector q^2 for both the TE and TM surface plasmons are in the region $[\max[\varepsilon_d, \varepsilon\mu - \gamma^2], \varepsilon\mu]$. If $\gamma = 0$, the condition for supporting both the TE and TM surface plasmons requires both negative permittivity and permeability, i.e. a DNM.

Here we propose a realistic metamaterial [32] design for experimental realization of the bianisotropic metamaterial that will support both TE and TM surface modes. The unit cell of the metamaterial is schematically shown in Figure 1D, which is equivalent to a pair of orthogonal split-ring resonators denoted by red and blue. Each split ring is equivalent to an LC circuit, with the gap and loop acting as a capacitor and an inductor, respectively. The bianisotropic property can be understood from the fields and current distribution for an z -polarized incident wave acting on the blue one, where the excited electric current j_z forms a magnetic dipole moment $-im_y$, and vice versa [29]. The coupling between the electric and magnetic fields results in bianisotropy. By calculating the two lowest bulk modes of the unit cell using CST Microwave Studio and fitting the equi-frequency surface (EFS) [29], we retrieve the effective parameters with $\boldsymbol{\varepsilon} = \text{diag}(5.89, 6.79, 6.79)$, $\boldsymbol{\mu} = \text{diag}(1, 1.13, 1.13)$, and $\gamma = 1.16$ at 8.7 GHz. The EFS for the bianisotropic material at 8.7 GHz is illustrated in Figure 2A. It consists of two ellipsoids of opposite helicity states. The dashed blue lines show the EFS of the normal dielectric material with $\varepsilon_d = 5.4$. By applying the boundary condition, i.e. matching the transverse components of the electric and magnetic fields across the interface, the dispersion of the surface modes can be numerically solved [31, 33], which are very close to two of the interception points of the two ellipsoids. Figure 2B gives an enlarged view of the region indicated by the black rectangle in Figure 2A, in which the highlighted blue and red points represent the pure TE and TM surface modes, respectively.

The dispersion of the surface modes for the realistic structure is calculated by full-wave simulation using the Eigenmode Solver of CST Microwave studio (see Supplementary Material), as shown in Figure 3A. We use 16 bianisotropic meta-unit cells on one side and a dielectric material of thickness $16P_x$ with $\varepsilon = 5.4$ on the other side. For the calculation of the dispersion along k_z , we fix $k_y = 2.38k_0$, which is outside the bulk mode. The lowest two modes are the surface modes existing at the bianisotropic metamaterial/dielectric material interface. The

highlighted blue point at the frequency of 8.73 GHz and red point at the frequency of 8.66 GHz in Figure 3A are the TE and TM surface modes, respectively. The corresponding magnetic energy E_m and the z -component of magnetic field H_z of the TM surface mode are shown in Figure 3B and C, respectively. The electric energy E_e and the z -component of electric field E_z of the TE surface mode are shown in Figure 3D and E, respectively. In both cases, we observe the confinement of the modes at the interface between the bianisotropic metamaterial and the dielectric material. It is also evident that the dominant field components for the two surface modes are TE and TM, respectively.

It should be noted that pure TM and TE modes exist in the lower and upper bands only along the k_y direction ($k_z = 0$), with the in-plane polarization of the two modes along the y - and z -axis, respectively. Away from this propagation direction, the surface modes are not pure

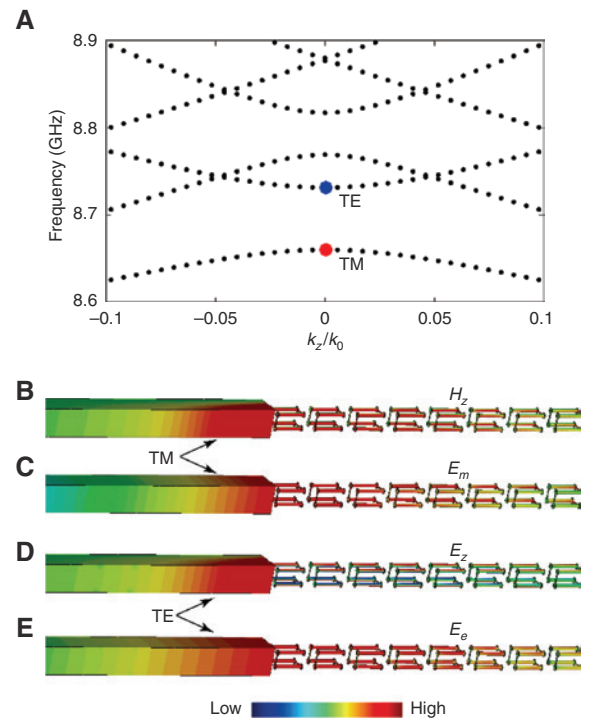


Figure 3: Demonstration of coexistence of TE and TM surface modes by CST Microwave Studio.

(A) Dispersion relation between frequency and wave vector of the y -component with fixed $k_z = 2.38k_0$. k_0 is the wave vector in vacuum at 8.7 GHz. The black and red lines are the SW modes at the bianisotropic material/dielectric material interface. The blue point at the frequency 8.73 GHz and the red point at the frequency 8.66 GHz are the TE and TM surface modes, respectively. The inset shows the two surface mode bands. (B) Magnetic energy (E_m) of the TM surface mode. (C) z -Component of the H-field of the TM surface mode. (D) Electric energy (E_e) of the TE surface mode. (E) z -Component of the E-field of the TE surface mode.

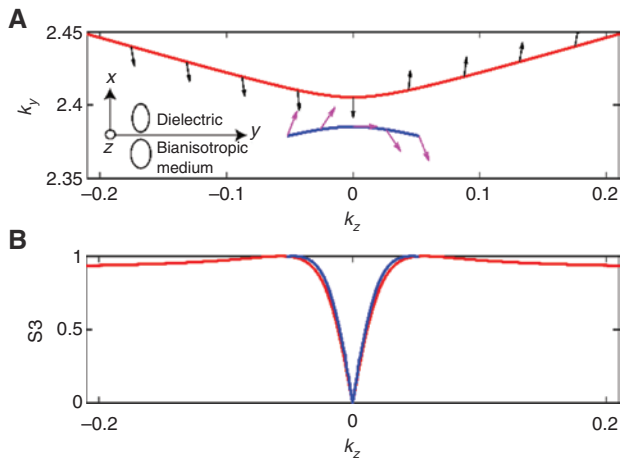


Figure 4: Polarization properties of the surface waves.

(A) In-plane polarization states of the two band surface waves at the dielectric material/bianisotropic metamaterial interface. The red and blue lines indicate the two surface arcs, respectively. The black and magenta arrows in the upper and lower bands denote the in-plane polarization direction, respectively. The inset picture shows that the polarization states on both side of the interface are elliptical and the in-plane polarization plane is perpendicular to the propagation plane. (B) Stokes parameters S_3 of the upper and lower bands of the surface wave in the bianisotropic metamaterial is plotted by red and blue lines, respectively.

TE and TM anymore, and they exhibit interesting spin texture along the surface arc. Numerically we calculate the in-plane polarization direction of the surface modes, as shown in Figure 4A. In addition, we calculate the Stokes parameters S_3 based on the magnetic field and the electric field for the upper and lower bands, respectively. The Stokes parameters of the surface modes are illustrated in Figure 4B. At $k_z = 0$, the Stokes parameters S_3 equal zero, corresponding to pure TE and TM surface modes. The Stokes parameter S_3 increase rapidly away from $k_z = 0$ and approximate to 1 on both ends, which may allow for spin-dependent excitation of the surface plasmons.

3 Conclusions

Both TE and TM surface modes are simultaneously supported at the interface of a bianisotropic metamaterial and a dielectric material. Comparing the dispersion relation of the surface modes, the bianisotropic metamaterial exhibits properties akin to those of a DNM, while the bianisotropic metamaterial is more likely realizable than DNM. We have proposed a realistic model for the realization of bianisotropic metamaterials. The surface

modes demonstrated here have potential applications in optical information processing and integrated photonic devices.

Acknowledgments: We acknowledge the support from the ERC Consolidator Grant (TOPOLOGICAL, Funder Id: <http://dx.doi.org/10.13039/501100000781>), the Horizon 2020 Action (Project No. 734578), the National Natural Science Foundation of China (grant 11604216), and the Chinese Scholarship Council Grant (No. 201606250059) to LX.

References

- [1] Shelby RA, Smith DR, Schultz S. Experimental verification of a negative index of refraction. *Science* 2001;292:77–9.
- [2] Fang N, Lee H, Sun C, Zhang X. Sub-diffraction-limited optical imaging with a silver superlens. *Science* 2005;308:534–7.
- [3] Liu Z, Lee H, Xiong Y, Sun C, Zhang X. Far-field optical hyperlens magnifying sub-diffraction-limited objects. *Science* 2007;315:1686.
- [4] Zhang X, Liu Z. Superlenses to overcome the diffraction limit. *Nat Mater* 2008;7:435–41.
- [5] Lu D, Liu Z. Hyperlenses and metalenses for far-field super-resolution imaging. *Nat Commun* 2012;3:1205.
- [6] Pendry JB, Schurig D, Smith DR. Controlling electromagnetic fields. *Science* 2006;312:1780–2.
- [7] Schurig D, Mock JJ, Justice BJ, et al. Metamaterial electromagnetic cloak at microwave frequencies. *Science* 2006;314:977–80.
- [8] Chen H, Wu B-I, Zhang B, Kong JA. Electromagnetic wave interactions with a metamaterial cloak. *Phys Rev Lett* 2007;99:063903.
- [9] Chen H, Chan CT, Sheng P. Transformation optics and metamaterials. *Nat Mater* 2010;9:387–96.
- [10] Shalaev VM. Optical negative-index metamaterials. *Nat Photon* 2007;1:41–8.
- [11] Larouche S, Tsai Y-J, Tyler T, Jokerst NM, Smith DR. Infrared metamaterial phase holograms. *Nat Mater* 2012;11:450–4.
- [12] Huang L, Chen X, Mühlenbernd H, et al. Three-dimensional optical holography using a plasmonic metasurface. *Nat Commun* 2013;4:1.
- [13] Ni X, Kildishev AV, Shalaev VM. Metasurface holograms for visible light. *Nat Commun* 2013;4:2807.
- [14] Zheng G, Mühlenbernd H, Kenney M, Li G, Zentgraf T, Zhang S. Metasurface holograms reaching 80% efficiency. *Nat Nanotechnol* 2015;10:308–12.
- [15] Wen D, Yue F, Li G, et al. Helicity multiplexed broadband metasurface holograms. *Nat Commun* 2015;6:8241.
- [16] Pendry JB, Martin-Moreno L, Garcia-Vidal FJ. Mimicking surface plasmons with structured surfaces. *Science* 2004;305:847–8.
- [17] Zhang S, Park YS, Li J, Lu X, Zhang W, Zhang X. Negative refractive index in chiral metamaterials. *Phys Rev Lett* 2009;102:023901.
- [18] Zhang X, Tian Z, Yue W, et al. Broadband terahertz wave deflection based on C-shape complex metamaterials with phase discontinuities. *Adv Mater* 2013;25:4567–72.
- [19] Cong L, Xu N, Han J, Zhang W, Singh R. A tunable dispersion-free terahertz metadvice with Pancharatnam–Berry-phase

- enabled modulation and polarization control. *Adv Mater* 2015;27:6630–6.
- [20] Smith DR, Padilla WJ, Vier DC, Nemat-Nasser SC, Schultz S. Composite medium with simultaneously negative permeability and permittivity. *Phys Rev Lett* 2000;84:4184–7.
- [21] Bliokh KY, Smirnova D, Nori F. Quantum spin Hall effect of light. *Science* 2015;348:1448–51.
- [22] Bekshaev AY, Bliokh KY, Nori F. Transverse spin and momentum in two-wave interference. *Phys Rev X* 2015;5:011039.
- [23] Van Mechelen T, Jacob Z. Universal spin-momentum locking of evanescent waves. *Optica* 2016;3:118–26.
- [24] Veselago VG. The electrodynamics of substances with simultaneously negative values of ϵ and μ . *Sov Phys Uspekhi* 1968;10:509–14.
- [25] Pendry JB. Negative refraction makes a perfect lens. *Phys Rev Lett* 2000;85:3966–9.
- [26] Baccarelli P, Burghignoli P, Lovat G, Paulotto S. Surface-wave suppression in a double-negative metamaterial grounded slab. *IEEE Antennas Wirel Propag Lett* 2003;2:269–72.
- [27] Shu W, Song J. Complete mode spectrum of a grounded dielectric slab with double negative metamaterials. *Prog Electromagn Res* 2006;65:103–23.
- [28] El-Khozondar HJ, El-Khozondar RJ, Shabat MM. Double-negative metamaterial optical waveguide behavior subjected to stress. *SPIE Photon Eur* 2008;8.
- [29] Guo Q, Gao W, Chen J, Liu Y, Zhang S. Line degeneracy and strong spin-orbit coupling of light with bulk bianisotropic metamaterials. *Phys Rev Lett* 2015;115:067402.
- [30] D'yakonov M. New type of electromagnetic wave propagating at an interface. *Sov Phys JETP* 1988; 67:714–6.
- [31] Xia L, Gao W, Yang B, et al. Stretchable photonic 'Fermi Arcs' in twisted magnetized plasma. *Laser Photon Rev* 2018;12:1700226.
- [32] Yang B, Guo Q, Tremain B, et al. Ideal Weyl points and helicoid surface states in artificial photonic crystal structures. *Science* 2018;359:1013–6.
- [33] Gao W, Lawrence M, Yang B, et al. Topological photonic phase in chiral hyperbolic metamaterials. *Phys Rev Lett* 2015;114:037402.

Supplementary Material: The online version of this article offers supplementary material (<https://doi.org/10.1515/nanoph-2019-0047>).